Diffusion Data for Silicate Minerals, Glasses, and Liquids

John B. Brady

1. INTRODUCTION

Diffusion is an integral part of many geologic processes and an increasing portion of the geologic literature is devoted to the measurement, estimation, and application of diffusion data. This compilation is intended to be a guide to recent experimentally-determined diffusion coefficients and, through the papers cited, to important older literature. To provide a context for the tables, a brief summary of the equations required for a phenomenological (macroscopic) description of diffusion follows. Although the equations for well-constrained experiments are relatively straightforward, the application of the resulting diffusion coefficients to complex geologic problems may not be straightforward. The reader is urged to read one or more diffusion texts [e.g., 99, 121, 32, 147, 135] before attempting to use the data presented here.

2. FORCES AND FLUXES

Diffusion is the thermally-activated, relative movement (flux) of atoms or molecules that occurs in response to forces such as gradients in chemical potential or temperature. Diffusion is spontaneous and, therefore, must lead to a net decrease in free

energy. For example, the movement of Δn_i moles of chemical component i from a region (II) of high chemical potential (μ_i^{II}) to a region (I) of lower chemical potential (μ_i^{I}) will cause the system Gibbs energy (G) to fall since

$$\Delta G^{I} + \Delta G^{II} = \Delta n_i \left(\frac{\partial G^{I}}{\partial n_i} \right)_{P,T,n_j} - \Delta n_i \left(\frac{\partial G^{II}}{\partial n_i} \right)_{P,T,n_j} \quad (1)$$

and using the definition of μ_i [139, p.128],

$$\Delta G^{Total} = \Delta n_i \left(\mu_i^{I} - \mu_i^{II} \right) < 0 . \quad (2)$$

Thus, a chemical potential gradient provides a thermodynamic force for atom movement.

On a macroscopic scale, *linear* equations appear to be adequate for relating each diffusive flux to the set of operative forces [137, p.45]. The instantaneous, one-dimensional, isothermal diffusive flux J_i^{R} (moles of i/m^{2}s) of component i in a single-phase, n-component system with respect to reference frame R may be described by

$$J_i^{R} = \sum_{j=1}^{n} -L_{ij}^{R} \left(\frac{\partial \mu_j}{\partial x} \right), \quad (3)$$

where x (m) is distance and the n^2 terms L_{ij}^{R} (moles of i/m·J·s) are "phenomenological diffusion coefficients" [36]. Because each component of the system may move in response to a gradient in the chemical potential of any other component, the complexity of describing diffusion in multicomponent systems rises

J. B. Brady, Department of Geology, Smith College, Northampton, MA 01063

rapidly with the number of components. Two impor-
tant results help limit this complexity. First, the iso-
thermal, isobaric Gibbs-Duhem equation [139, p.
134]

$$\sum_{i=1}^{n} n_i \, d\mu_i = 0 \tag{4}$$

for the single phase in which the diffusion occurs
reduces the number of independent gradients to (n-1)
and the number of diffusion coefficients to $(n-1)^2$.
Second, Onsager [132, 133] showed that if the
forces, fluxes, components, and reference frame are
properly chosen, the matrix of coefficients relating the
forces and fluxes is symmetrical

$$L_{ij}^{R} = L_{ji}^{R}, \tag{5}$$

reducing the number of independent diffusion
coefficients to (2n-1).

Although equations (3)-(5) are theoretically satisfy-
ing, they are *not* generally used to describe diffusion
experiments, in part because chemical potential
gradients are not directly measurable in most cases.
Fisher [51], Joesten [94, 96, 97], and others [e.g.,
55, 98, 16, 1] have applied these equations success-
fully in modeling the diffusion evolution of coronas
and other textures in some rocks. However, most
workers use empirical equations related to (3) that
involve measurable compositions C_j (moles of j/m^3)

$$J_i^{R} = \sum_{j=1}^{n-1} -D_{ij}^{R} \left(\frac{\partial C_j}{\partial x} \right) \tag{6}$$

[134]. Only (n-1) compositions are independent, but
unfortunately $D_{ij}^{R} \neq D_{ji}^{R}$ so that $(n-1)^2$ diffusion
coefficients D_{ij}^{R} (m^2/s) are needed for (6).

The most obvious simplification of (6) is to limit the
number of components to 2 and, therefore, the num-
ber of required diffusion coefficients to 1. Most
experimentalists achieve this by their experimental
design. The next two sections present definitions and
equations used to describe these binary (2-compo-
nent) experiments. Additional ways to simplify the
treatment of multicomponent systems are addressed in
Section 5.

3. FICK'S LAWS

Adolf Fick's [50] empirical equations were used to
describe binary diffusion experiments long before the
more general equations (3) and (6) were developed.
Fick's First Law

$$J_i = -D_i \left(\frac{dC_i}{dx} \right) \tag{7}$$

relates the instantaneous flux J_i (moles of i/m^2s) of
component i to the one-dimensional gradient of the
concentration of i, dC_i/dx (moles of i/m^4), and
defines the diffusion coefficient D_i (m^2/s). However,
unless the experiment attains a steady state, time (t) is
also a variable and a continuity equation (Fick's
Second Law)

$$\left(\frac{\partial C_i}{\partial t} \right)_x = \left(\frac{\partial}{\partial x} \left[D_i \left(\frac{\partial C_i}{\partial x} \right)_t \right] \right)_t \tag{8}$$

must be solved. If D_i is not a function of composition
(C_i) and, therefore, not a function of position (x),
then equation (4) may be simplified to

$$\left(\frac{\partial C_i}{\partial t} \right)_x = D_i \left(\frac{\partial^2 C_i}{\partial x^2} \right)_t, \tag{9}$$

which has many analytical solutions [6, 99, 17, 32].

Some commonly used solutions to (5) for planar
geometries are given in Table 1 and two of these are
shown graphically in Figure 1. All of the equations
(7)-(13) implicitly assume constancy of volume, for
which the fixed laboratory reference frame is a mean
volume reference frame, and must be modified if the
sample volume does change [10]. Similar analytical
solutions exist for related boundary conditions and/or
other geometries, notably spherical and cylindrical
cases. More complicated boundary conditions and
geometries may require numerical approximation [32,
Chap. 8].

It is clear from Table 1 and Figure 1 that the
parameter $\sqrt{D_i t}$ may be used to characterize the extent
of diffusion. In semi-infinite cases such as (10) and
(11), the distance x that has attained a particular value
of C_i after time t is proportional to $\sqrt{D_i t}$. In finite

Table 1. Commonly-used solutions to equation (9)

Boundary Conditions	Solution	
Thin-film Solution $\begin{cases} C_i \to C0 \text{ for } |x| > 0 \text{ as } t \to 0 \\ C_i \to \infty \text{ for } x = 0 \text{ as } t \to 0 \end{cases}$	$\left(\dfrac{C_i - C0}{\alpha}\right) = \dfrac{1}{2\sqrt{\pi D_i t}} \exp\left(\dfrac{-x^2}{4 D_i t}\right) \quad \text{where} \quad \alpha \equiv \int_{-\infty}^{+\infty}(C_i - C0)\,dx$	(10)
Semi-infinite Pair Solution $\begin{cases} C_i = C0 \text{ for } x > 0 \text{ at } t = 0 \\ C_i = C1 \text{ for } x < 0 \text{ at } t = 0 \end{cases}$	$\left(\dfrac{C_i - C0}{C1 - C0}\right) = \dfrac{1}{2}\,\mathrm{erfc}\left(\dfrac{x}{2\sqrt{D_i t}}\right)$	(11)
Finite Pair Solution $\begin{cases} C_i = C1 \text{ for } 0 < x < h \text{ at } t = 0 \\ C_i = C0 \text{ for } h < x < L \text{ at } t = 0 \\ (\partial C_i / \partial x)_t = 0 \text{ for } x = 0\,\&\,L \end{cases}$	$\left(\dfrac{C_i - C0}{C1 - C0}\right) = \dfrac{h}{L} + \dfrac{2}{\pi}\sum_{n=1}^{\infty}\dfrac{1}{n}\sin\left(\dfrac{n\pi h}{L}\right)\exp\left(\dfrac{-D_i n^2 \pi^2 t}{L^2}\right)\cos\left(\dfrac{n\pi x}{L}\right)$	(12)
Finite Sheet - Fixed Surface Composition $\begin{cases} C_i = C0 \text{ for } -L < x < L \text{ at } t = 0 \\ C_i = C1 \text{ for } x = 0\,\&\,L \text{ at } t > 0 \end{cases}$	$\left(\dfrac{C_i - C0}{C1 - C0}\right) = 1 - \dfrac{4}{\pi}\sum_{n=0}^{\infty}\dfrac{-1^n}{2n+1}\exp\left(\dfrac{-D_i(2n+1)^2\pi^2 t}{4L^2}\right)\cos\left(\dfrac{(2n+1)\pi x}{2L}\right)$	(13)

cases such as (12) and (13), the fractional extent of completion of homogenization by diffusion is proportional to $\sqrt{D_i t}$. These $\sqrt{D_i t}$ relations provide important tests that experimental data must pass if diffusion is asserted as the rate-controlling process. They also provide simple approximations to the limits of diffusion when applying measured diffusion coefficients to specific problems [147].

4. DIFFUSION COEFFICIENTS

In general, one must assume that D_i *is* a function of C_i. Therefore, equations (9)-(13) may be used with confidence only if C_i does not change appreciably during the experiment. This is accomplished either (a) by using a measurement technique (typically involving radioactive tracers) that can detect very small changes in C_i, or (b) by using diffusional exchange of stable isotopes of the same element that leave the element concentration unchanged. Approach (a) yields a "tracer diffusion coefficient" for the element that is specific to the bulk composition studied. Approach (b) yields a "self-diffusion coefficient" for the isotopically doped element that is also specific to the bulk chemical composition. Both approaches generally ignore the opposite or exchange flux that must occur in dominantly ionic phases such

as silicate minerals, glasses, and liquids.

If C_i does change significantly in the experiment and D_i is a function of C_i, observed compositional profiles might not match the shape of those predicted by (9)-(13). In such cases the D_i calculated with these equations will be at best a compositional "average" and equation (8) should be considered. Experiments in which composition does change significantly are often termed "interdiffusion" or "chemical diffusion" experiments. A commonly-used analytical solution to (8), for the same boundary conditions as for equation (11), was obtained by Matano [122] using the Boltzmann [8] substitution $(\chi \equiv x / \sqrt{t})$:

$$D_i(C2) = \frac{-1}{2t}\left(\frac{dx}{dC_i}\right)_{C_i = C2} \int_{C_i = C0}^{C_i = C2} x\,dC_i . \tag{14}$$

Equation (14) can be evaluated numerically or graphically from a plot of $(C_i - C0)/(C1 - C0)$ versus x, where the point $x = 0$ (the Matano interface) is selected such that

$$\int_{C_i = C0}^{C_i = C1} x\,dC_i = 0 \tag{15}$$
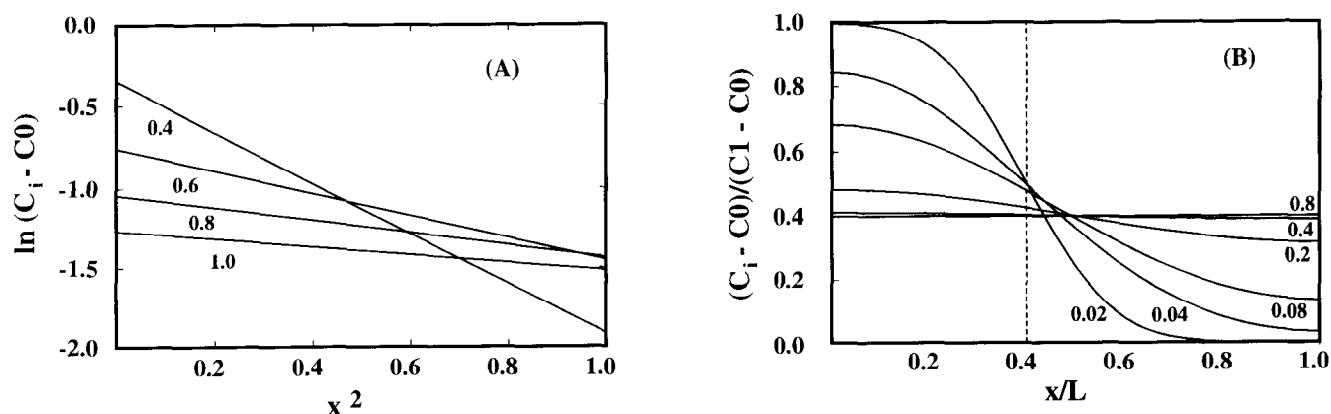
Figure 1. Graphical solutions to equation (9). (A) The "thin film" solution of equation (10) is shown with $\alpha=1$ for various values of $\sqrt{D_i t}$ (labels on lines). Plotting $\ln(C_i - C0)$ as a function of x^2 at any time yields a straight line of slope $-1/(4D_i t)$. (B) The "finite pair" solution of equation (12) is shown for h/L=0.4 and various values of Dt/L^2 (labels on curves). Plotting $(C_i -C0)/(C1 - C0)$ as a function of x/L normalizes all cases to a single dimensionless graph. The initial boundary between the two phases is marked by a dashed vertical line.

[32, p.230-234]. For binary, cation exchange between ionic crystals, the Matano interface is the original boundary between the two crystals. Diffusion experiments that follow the Boltzmann-Matano approach have the advantage of determining D_i as a function of C_i and the disadvantage of risking the complications of multicomponent diffusion, for which neither (8) nor (14) is correct.

Darken [35] and Hartley and Crank [83] showed that for electrically neutral species, the binary $(A \leftrightarrow B)$ interdiffusion coefficients $(D_{AB_{-1}})$ obtained in a Boltzmann-Matano type experiment and the tracer diffusion coefficients (D_A^* and D_B^*) for the interdiffusing species are related by

$$D_{AB_{-1}} = \left(N_B D_A^* + N_A D_B^*\right)\left[1 + \left(\frac{\partial \ln \gamma_A}{\partial \ln N_A}\right)_{P,T}\right], \quad (16)$$

where N_A is the mole fraction and γ_A the molar activity coefficient of component A. Darken developed his analysis in response to the experiments of Smigelskas and Kirkendall [148], who studied the interdiffusion of Cu and Zn between Cu metal and $Cu_{70}Zn_{30}$ brass. Smigelskas and Kirkendall observed that Mo wires (inert markers) placed at the boundary between the Cu and brass moved in the direction of the brass during their experiments, indicating that more Zn atoms than Cu atoms crossed the boundary. Darken's analysis showed that in the presence of inert markers the

independent fluxes and, therefore, the "tracer" diffusion coefficients of Cu and Zn can be determined in addition to the interdiffusion coefficient $D_{CuZn_{-1}}$.

A similar analysis for binary cation interdiffusion $(AZ \leftrightarrow BZ$ where AZ represents $A_z^{+a}Z_a^{-z}$ and BZ represents $B_z^{+b}Z_b^{-z})$ in appreciably ionic materials such as silicate minerals yields [5, 112, 113, 10]:

$$D_{A_b B_{-a}} = \left[\frac{\left(D_{AZ}^*\right)\left(D_{BZ}^*\right)(aN_{AZ} + bN_{BZ})^2}{\left(a^2 N_{AZ}D_{AZ}^* + b^2 N_{BZ}D_{BZ}^*\right)}\right]\left[1 + \left(\frac{\partial \ln \gamma_{AZ}}{\partial \ln N_{AZ}}\right)_{P,T}\right], \quad (17)$$

which requires vacancy diffusion if $a \neq b$. If a=b, then (17) simplifies to

$$D_{AB_{-1}} = \left[\frac{\left(D_{AZ}^*\right)\left(D_{BZ}^*\right)}{\left(N_{AZ}D_{AZ}^* + N_{BZ}D_{BZ}^*\right)}\right]\left[1 + \left(\frac{\partial \ln \gamma_{AZ}}{\partial \ln N_{AZ}}\right)_{P,T}\right] \quad (18)$$

[121]. This expression permits interdiffusion coefficients to be calculated from more-easily-measured tracer diffusion coefficients. For minerals that are not

ideal solutions, the "thermodynamic factor" in brackets on the right side of (16)-(18) can significantly change the magnitude (and even the sign!) of interdiffusion coefficients from those expected for an ideal solution [12, 25].

5. MULTICOMPONENT DIFFUSION

Rarely is diffusion in geologic materials binary. Multicomponent diffusion presents the possibility that diffusive fluxes of one component may occur in response to factors not included in (7)-(18), such as gradients in the chemical potentials of other components, coupling of diffusing species, etc. In these cases, equation (6) or (3) must be used. The off-diagonal (i≠j) diffusion coefficients, D_{ij}^R or L_{ij}^R, are unknown for most materials and most workers are forced to assume (at significant peril!) that they are zero. Garnet is the one mineral for which off-diagonal diffusivities are available [19, 20] and they were found to be relatively small.

One approach used by many is to treat diffusion that is one-dimensional in real space as if it were one-dimensional in composition space. This approach was formalized by Cooper and Varshneya [28, 30] who discuss diffusion in ternary glasses and present criteria to be satisfied to obtain "effective binary diffusion coefficients" from multicomponent diffusion experiments. In general, diffusion coefficients obtained with this procedure are functions of both composition and direction in composition space. Another approach, developed by Cullinan [33] and Gupta and Cooper [75, 29], is to diagonalize the diffusion coefficient matrix for (6) through an eigenvector analysis. Although some simplification in data presentation is achieved in this way, a matrix of diffusion coefficients must be determined before the analysis can proceed.

Lasaga [105, see also 161] has generalized the relationship (17) to multicomponent minerals. The full expression is quite long, but simplifies to

$$D_{ij} = D_i^* \delta_{ij} - \left(\frac{D_i^* C_i z_i z_j}{\sum\limits_{k=1}^{n} D_k^* C_k z_k^2} \right) \left(D_j^* - D_n^* \right) \qquad (19)$$

if the solid solution is thermodynamically ideal. In (19) z_i is the charge on cation i, $\delta_{ij} = 1$ if i=j, and $\delta_{ij} = 0$ if i≠j. This approach, using tracer diffusion

coefficients D_i^* to calculate multicomponent interdiffusion coefficient matrices, and its inverse offer the most hope for diffusion analysis of multicomponent problems [115, 19, 20]. It should be noted in using equations (16)-(19) that the tracer diffusivities themselves may be functions of bulk composition.

6. EXPERIMENTAL DESIGN

A few additional considerations should be mentioned regarding the collection and application of diffusion data.

• In anisotropic crystals, diffusion may be a function of crystallographic orientation and the diffusion coefficient becomes a second rank tensor. The form of this tensor is constrained by point group symmetry and the tensor can be diagonalized by a proper choice of coordinate system [131].

• Vacancies, dislocations, and other crystal defects may have profound effects on diffusion rates [e.g., 121, 164]. Therefore, it is essential that the mineral being studied is well-characterized. If the mineral, liquid, or glass contains a multivalent element like Fe, then an equilibrium oxygen fugacity should be controlled or measured because of its effect on the vacancy concentration.

• Diffusion in rocks or other polycrystalline materials may occur rapidly along grain boundaries, crystal interfaces, or surfaces and will not necessarily record intracrystalline diffusivities. Experiments involving grain-boundary diffusion [e.g., 102, 103, 11, 47, 49, 95, 154, 13, 158] are beyond the scope of this summary. If polycrystalline materials are used in experiments to measure "intrinsic" or "volume" diffusion coefficients, then the contributions of "extrinsic" grain-boundary diffusion must be shown to be negligible.

• Water can have a major effect on diffusion in many geologic materials, even in small quantities [e.g., 73, 150, 46, 167, 71]. If water is present, water fugacities are an essential part of the experimental data set.

• Because many kinetic experiments cannot be "reversed," every effort should be made to demonstrate that diffusion is the rate-controlling process. Important tests include the $\sqrt{D_i t}$ relations noted in equations (10)-(13) and the "zero time experiment." The $\sqrt{D_i t}$ test can be used if data are gathered at the same physical conditions for at least two times, preferably differing by a factor of four or more. The often-overlooked "zero time experiment,"

which duplicates the sample preparation, heating to the temperature of the experiment, quenching (after "zero time" at temperature), and data analysis of the other diffusion experiments, commonly reveals sources of systematic errors.

These and other important features of diffusion experiments are described in Ryerson [141].

7. DATA TABLE

Due to space limitations, the data included in this compilation have been restricted to comparatively recent experimental measurements of diffusion coefficients for silicate minerals, glasses, and liquids. Many good, older data have been left out, but can be found by following the trail of references in the recent papers that are included. Older data may also be found by consulting the compilations of Freer [56, 57], Hofmann [86], Askill [2], and Harrop [81]. Some good data also exist for important non-silicate minerals such as apatite [157, 23, 45] and magnetite-titanomagnetite [65, 136, 59], but the silicate minerals offered the clearest boundary for this paper.

Almost all of the data listed are for tracer or self-diffusion. Interdiffusion (chemical diffusion) experiments involving minerals are not numerous and interdiffusion data sets do not lend themselves to compact presentation. Interdiffusion data for silicate liquids and glasses are more abundant, but are not included [see 156, 3, 4]. Neither are non-isothermal (Soret) diffusion data [see 108]. Diffusion data listed for silicate glasses and liquids have been further restricted to bulk compositions that may be classified as either basalt or rhyolite.

Because diffusion is thermally activated, coefficients for diffusion by a single mechanism at different temperatures may be described by an Arrhenius equation

$$D = D_o \exp\left(\frac{-\Delta H}{RT}\right) \tag{20}$$

and fit by a straight line on a graph of log D (m²/s) as a function of 1/T (K⁻¹) [147, Chap. 2]. Log D_0 (m²/s) is the intercept of the line on the log D axis (1/T = 0). $\Delta H/(2.303 \cdot R)$ is the slope of the line where R is the gas constant (8.3143 J/mole·K) and

ΔH (J/mole) is the "activation energy." D_0 and ΔH have significance in the atomic theory of diffusion [see 32, 121] and may be related for groups of similar materials [162, 82, 106].

Diffusion data are listed in terms of ΔH and log D_0 and their uncertainties. In many cases data were converted to the units (kJ, m²/s) and form (log D_0) of this compilation. Logarithms are listed to 3 decimal places for accurate conversion, even though the original data may not warrant such precision. No attempt was made to reevaluate the data, the fit, or the uncertainties given (or omitted) in the original papers. Also listed are the conditions of the experiment as appropriate including the temperature range, pressure range, oxygen fugacity, and sample geometry. Extrapolation of the data using (20) to conditions outside of the experimental range is not advisable. However, for ease of comparison log D is listed for a uniform temperature of 800°C (1200°C for the glasses and liquids), even though this temperature may be outside of the experimental range. Use these tabulated log D numbers with caution.

Finally, a sample "closure temperature" (T_c) has been calculated for the silicate mineral diffusion data. The closure temperature given is a solution of the Dodson [38] equation

$$\left(\frac{\Delta H}{RT_c}\right) = \ln\left(\frac{-55 \ RT_c^2 D_o}{a^2 \Delta H(dT/dt)}\right) \tag{21}$$

for a sphere of radius a=0.1 mm and a cooling rate (dT/dt) of 5 K/Ma. The example closure temperatures were included because of the importance of closure temperatures in the application of diffusion data to petrologic [107] and geochronologic [123, Chap. 5] problems. Note that other closure temperatures would be calculated for different crystal sizes, cooling rates, and boundary conditions.

Mineral, Glass, or Liquid	Orienta-tion	Diffusing Component	Temperature Range (°C)	P (MPa)	O_2 (MPa)	ΔE_a (kJ/mole)	log D_0 (or D) (m²/s)	log D 800°C	"T_c" (°C)	Experiment/Comments	Ref.
β-quartz (SiO_2)	//c-axis	H	700-900	890-1550	UB	200 (±20)	-0.854	-10.6	188	Exchange with water-bearing fluid, "bulk" IR spectra	[104]
β-quartz (SiO_2)	//c-axis	^{18}O	600-800	100	UB	142 (±4)	-10.398(±0.272)	-17.3	282	Exchange with ^{18}O-enriched water, ion probe profiles	[68]
β-quartz (SiO_2)	⊥ c-axis	^{18}O	600-800	100	UB	234 (±8)	-8.000 (±2.239)	-19.4	498	Exchange with ^{18}O-enriched water, ion probe profiles	[68]
β-quartz (SiO_2)	//c-axis	^{18}O	700-850	100	UB/ NO	138.5(±19.1)	-10.680(±0.955)	-17.4	278	Exchange with ^{18}O-enriched water, ion probe profiles	[37]
β-quartz (SiO_2)	⊥ c-axis	^{18}O	700-850	100	UB/ NO	203.7(+2.3)	-9.413(±0.151)	-19.3	462	Exchange with ^{18}O-enriched water, ion probe profiles	[37]
β-quartz (SiO_2)	//c-axis	^{18}O	745-900	10	CO_2	159(±13)	-3.678(±0.132)	-11.4	146	Exchange with $C^{18}O_2$ gas, ion probe profiles	[146]
α-quartz (SiO_2)	//c-axis	^{18}O	450-590	100	UB	243 (±17)	-4.538	-16.4	389	Exchange with ^{18}O-enriched water, ion probe profiles	[48]
β-quartz (SiO_2)	⊥ (101)	^{30}Si	912-1028	0.1	air	230	-9.699	-20.9	570	Surface thin film of ^{30}Si, ion probe profile	[69]
β-quartz (SiO_2)	//c-axis	"^3H_2O"	720-850	0.061	UB	100 (±1.7)	-10.194(±0.099)	-15.1	115	Exchange with tritiated water vapor, serial section profiles, conc. dependent D	[145]
β-quartz (SiO_2)	//c-axis	"H_2O"	900	1500	NO	n.d.	(D=10^{-11})			Exchange with water/ D_2O, bulk analysis, IR spectra	[140]
adularia ($Or_{97.6}Ab_{1.8}An_{0.5}$)	⊥ (001)	^{18}O	350-700	100	UB	107 (±5)	-11.346(±0.301)	-16.6	178	Exchange with ^{18}O-enriched water, ion probe profiles	[66]
adularia ($Or_{97.6}Ab_{1.8}An_{0.5}$)	⊥ (001)	^{18}O	650	5-1500	WM NNO	see paper - D varies w/f_{H2O}	independent of f_{O2}, f_{H2}, a_{H+}, P			Exchange with ^{18}O-enriched water, ion probe profiles	[46]
albite (low) ($Ab_{98}Or_{1.7}An_{1.2}$)	⊥ (001)	^{18}O	350-700	100	UB	89.1 (±5.0)	-12.636(±0.019)	-17.0	146	Exchange with ^{18}O-enriched water, ion probe profiles	[66]
anorthite ($An_{97}Ab_3$)	⊥ (001)	^{18}O	850-1300	0.1	O_2	236 (±8)	-9.000 (±0.349)	-20.5	553	Exchange with $^{18}O_2$ gas (+10% Ar), ion probe profile	[42]
anorthite ($An_{94}Ab_4$)	//[010]	^{18}O	1000-1300	0.1	(CO)/ (CO_2)	162 (±36)	-12.076(±1.337)	-20.0	439	Exchange with ^{18}O-enriched gas, ion probe profile	[143]
anorthite ($An_{95.3}Ab_{4.3}Or_{0.4}$)	⊥ (001)	^{18}O	350-800	100 "wet"	UB	109.6 (4.6)	-10.857±(0.021)	-16.2	172	Exchange with ^{18}O-enriched water, ion probe profiles	[66]
orthoclase ($Or_{94}Ab_6$)	powder	^{22}Na	500-800	200	UB	220.5 (+4.6)	-3.050 (±0.243)	-13.8	287	Exchange with brine, bulk analysis, cylindrical model	[53]
microcline (max) (Or_{100})	powder	^{22}Na	600-800	200	UB	80 (±8)	-9.636	-13.5	26	Exchange with $^{22}NaCl$ solution, sphere model	[109]
albite (low) ($Ab_{98}Or_{1.4}An_{0.6}$)	powder	^{22}Na	300-800	200	UB	176 (±8)	-4.903 (±0.814)	-13.5	218	Exchange with $^{22}NaCl$ solution, cylindrical model	[101] [163]

Mineral, Glass, or Liquid	Orienta-tion	Diffusing Component	Temperature Range (°C)	P (MPa)	O_2 (MPa)	ΔE_a (kJ/mole)	$\log D_0$ (or D) (m^2/s)	$\log D$ 800°C	"T_c" (°C)	Experiment/Comments	Ref.
orthoclase ($Or_{94}Ab_6$)	powder	^{40}Ar	500-800	200	UB	180.3 (±4.6)	-5.854 (±0.259)	-14.6	256	Ar loss into brine, bulk analysis, spherical model	[52]
microcline (max) (Or_{100})	powder	^{40}K	600-800	200	UB	293 (±8)	-1.874	-16.1	428	Exchange with ^{40}KCl solution, sphere model	[109]
albite (low) ($Ab_{98}Or_{1.4}An_{0.6}$)	powder	^{40}K	600-800	200	UB	172 (±25)	-8.125 (±0.337)	-16.5	301	Exchange with ^{40}KCl solution, cylindrical model	[101] [163]
orthoclase ($Or_{94}Ab_6$)	powder	^{41}K	600-800	200	UB	285.4 (±3.8)	-2.793 (±0.190)	-16.7	439	Exchange with brine, bulk analysis, cylindrical model	[53]
orthoclase ($Or_{94}Ab_6$)	//c-axis	^{87}Rb	625-800	100	UB	339 (±33)	-2.000 (±1.800)	-18.5	541	Exchange w/Rb-Sr-enriched water, ion probe profiles	[63]
albite (Ab_{98})	⊥ (001)	^{86}Sr	570-1080	0.1	air	272	-4.509	-17.7	465	Thin film of ^{86}Sr, ion probe profile, other plag in progress	[64]
orthoclase ($Or_{94}Ab_6$)	//c-axis	^{84}Sr or ^{86}Sr	625-900	100	UB	167 (±17)	-11.000(±0.900)	-19.1	405	Exchange w/Rb-Sr-enriched water, ion probe profiles	[63]
orthoclase (Or_{93})	⊥ (001)	SrAl-KSi interdiffusion	725-1075	0.1	air	284.1 (±6.7)	-6.224 (±0.302)	-20.1	568	Exchange w/Sr-Al-Si-O powder, Rutherford Back. Spec	[24]
anothoclase ($Ab_{68}Or_{27}An_5$)	⊥ (001)	SrAl-KSi interdiffusion	725-1075	0.1	air	373.7(±19.2)	-1.648 (±0.913)	-19.8	609	Exchange w/Sr-Al-Si-O powder, Rutherford Back. Spec	[24]
anothoclase ($Ab_{68}Or_{27}An_5$)	⊥ (010)	SrAl-KSi interdiffusion	725-1075	0.1	air	372.8(±20.1)	-2.346 (±0.951)	-20.5	634	Exchange w/Sr-Al-Si-O powder, Rutherford Back. Spec	[24]
anorthite (Ab_6An_{93})	⊥ (010)	Sr-Ca interdiffusion	725-1075	0.1	air	329.7(±22.6)	-5.415 (±1.037)	-21.5	660	Exchange w/Sr-Al-Si-O powder, Rutherford Back. Spec	[24]
albite (low) ($Ab_{98}Or_{1.4}An_{0.6}$)	//c-axis	^{84}Sr	640-800	100	UB	247 (±25)	-5.600 (±1.300)	-17.6	437	Exchange w/Rb-Sr-enriched water, ion probe profiles	[63]
adularia ($Or_{89.6}$) - albite ($Ab_{98.6}$)	⊥ (001) (couple)	K-Na interdiffusion	900-1000	1500	UB	n.d.	(D=10^{-17} to 10^{-15})			Microprobe profile, composition dependence, anisotropy	[25]
albite (Ab_{92}) exsolved ($An_{0/26}$)	⊥ ($0\bar{4}1$) (couple)	CaAl-NaSi interdiffusion	900-1050	1500 "wet"	MH	303 (±35)	-7.523 (±0.300)	-22.3	691	Average D from lamellar homogenization experiments	[114]
bytownite (An_{80}) exsolved ($An_{70/90}$)	⊥ ($03\bar{1}$) (couple)	CaAl-NaSi interdiffusion	1100-1400	0.1	air	516.3 (±19)	-2.959 (±0.662)	-28.1	1011	Average D from lamellar homogenization experiments	[74]
bytownite (An_{80}) exsolved ($An_{70/90}$)	⊥ ($03\bar{1}$) (couple)	CaAl-NaSi interdiffusion	900-975 1000-1050	1500 "wet"	MH	-317 (±35) -103	-4.959 (±0.300) -15.398	-20.4 -20.4	604 350	Average D's from lamellar homogenization experiments	[114]
K-feldspar (Or_{93})	⊥ (010)	Pb-? interdiffusion	750-1050	0.1	UB	301.7(±11.3)	-6.000 (+0.519)	-20.7	609	Exchange with PbS powder, Rutherford backscattering	[21]
K-feldspar (Or_{93})	⊥ (001)	Pb-? interdiffusion	750-1050	0.1	UB	306.7(±26.8)	-4.886 (±1.176)	-19.8	573	Exchange with PbS powder, Rutherford backscattering	[21]
Oligoclase (An_{23})	⊥ (010)	Pb-? interdiffusion	750-1050	0.1	UB	364.5(±12.1)	-2.921 (±0.540)	-20.7	638	Exchange with PbS powder, Rutherford backscattering	[21]
Oligoclase (An_{23})	⊥ (001)	Pb-? interdiffusion	750-1050	0.1	UB	226.0(±9.2)	-8.387 (±0.415)	-19.4	489	Exchange with PbS powder, Rutherford backscattering	[21]

Mineral, Glass, or Liquid	Orienta-tion	Diffusing Component	Temperature Range (°C)	P (MPa)	O_2 (MPa)	ΔE_a (kJ/mole)	$\log D_0$ (or D) (m^2/s)	$\log D$ 800°C	"T_c" (°C)	Experiment/Comments	Ref.
nepheline	powder	^{18}O	1000-1300	0.1	CO_2	104.6(±10.5)	-12.229	-17.3	199	Exchange with CO_2, spherical model, bulk analysis	[27]
biotite (see paper for comp.)	powder	^{18}O	500-800	100 "wet"	UB/ NO	142 (±8)	-9.041	-16.0	233	Exchange with ^{18}O-enriched water, bulk analysis, cylindrical model, ion probe too	[54]
phlogopite (see paper for comp.)	powder	^{18}O	600-900	100 "wet"	UB/ NO	176 (±13)	-7.854	-16.4	305	Exchange with ^{18}O-enriched water, bulk analysis, cylindrical model, ion probe too	[54]
phlogopite (Ann_4) (see paper for comp.)	powder	^{40}Ar	600-900	200, 1500 "wet"	UB/ NO	242 (±11)	-4.125 (±0.514)	-15.9	373	Degassing into water, bulk analysis, cylindrical model, ($\Delta V_a \cong 0$ m^3/mole)	[62] [67]
biotite (Ann_{56}) (see paper for comp. reference)	powder	^{40}Ar	600-750	100, 1400 "wet"	GM, QFM	197 (±9)	-5.114 (±0.614)	-14.7	281	Degassing into water, bulk analysis, cylindrical model ($\Delta V_a = 1.4 \times 10^{-5}$ m^3/mole)	[77]
biotite	powder	^{41}K	450-700	200 "wet"	UB/ NO	88				Exchange with ^{41}KCl solution, bulk analysis & ion probe, cylindrical model	[87] [88]
chlorite (sheridanite) (see paper)	powder	^2H	500-700	200 & 500	UB/ NO	171.7	-5.21	-13.6	214	Enchange with ^2H-selected water, bulk analysis, cylindrical model	[72]
mucovite	powder	^2H	450-750	200 & 400	UB	121.3	-7.98	-13.9	133	Enchange with ^2H-selected water, bulk analysis, cylindrical model	[70]
muscovite (see paper for comp.)	powder	^{18}O	512-700	100 "wet"	UB/ NO	163 (±21)	-8.114	-16.1	273	Exchange with ^{18}O-enriched water, bulk analysis, cylindrical model, ion probe too	[54]
tremolite (see paper for comp.)	// c-axis	^{18}O	650-800	100 "wet"	UB/ NO	163 (±21)	-11.699(±1.204)	-19.6	424	Exchange with ^{18}O-enriched water, ion probe profiles	[44]
hornblende (see paper for comp.)	// c-axis	^{18}O	650-800	100,20 2000 "wet"	UB/ NO	172 (±25)	-11.000(±1.322)	-19.4	421	Exchange with ^{18}O-enriched water, ion probe profiles, anisotropy, pressure depend.	[44]
richterite (see paper for comp.)	// c-axis	^{18}O	650-800	100 "wet"	UB/ NO	239 (±8)	-7.523 (±0.452)	-19.1	490	Exchange with ^{18}O-enriched water, ion probe profiles	[44]
hornblende (see paper for comp.)	powder	^{40}Ar	750-900	100 "wet"	UB or NO	268.2 (±7.1)	-5.620 (±0.506)	-18.7	497	Degassing into water, bulk analysis, spherical model	[76]
tremolite	// c-axis	Sr	800	200 "wet"	UB/ NO		D=1x10^{-21}			Thin film solution, ion probe profile	[9]

Mineral, Glass, or Liquid	Orientation	Diffusing Component	Temperature Range (°C)	P (MPa)	O₂ (MPa)	ΔE_a (kJ/mole)	log D_0 (or D) (m²/s)	log D 800°C	"T_c" (°C)	Experiment/Comments	Ref.
orthopyroxene	powder	Fe-Mg interdiffusion	600-800	0.1	-12.2- -17.9	233	-9.432	-20.8	564	Calculated from disordering experiments [7]	[60]
diopside $(Ca_{.92}Mg_{.98}Fe_{.10})$	powder	He "apparent diffusivity"	700-1400	0.0	UB	290 (±40)	-1.9 (±1.2)	-16.0	422	Degassing experiment, spherical model, fractures!	[151]
diopside (synthetic)	powder	^{18}O	1150-1350	0.1	CO_2	59(±13)	-14.886(±0.520)	-17.7	71	Exchange with CO_2, spherical model, bulk analysis	[130]
diopside $(Wo_{50.6} En_{48.3}Fs_{1.1})$	// c-axis	^{18}O	1100-1250	0.1	NNO	-457 (±26)	-3.367 (±0.934)	-25.6	888	Exchange with ^{18}O-enriched gas, ion probe profiles	[143]
diopside ("essentially pure")	// c-axis	^{18}O	700-1250	100 "wet"	UB	226 (±21)	-9.824	-20.8	562	Exchange with ^{18}O-enriched water, ion probe profiles	[43]
diopside ("essentially pure")	⊥ c-axis	^{18}O	700-1250	100 "wet"	UB	226	-11.553	-22.6	671	Exchange with ^{18}O-enriched water, ion probe profiles	[43]
diopside $(Na_{.04} Ca_{.96}Mg_{.96}Fe_{.05} Al_{.06}Si_{1.96}O_6)$	// c-axis	Al-? interdiffusion	1180	0.1	$P(O_2)$ $=10^{-14}$	n.d.	$(D=3.2(±0.7)$ $x10^{-21})$			Thin film of amorphous $CaAl_2SiO_6$, $^{27}Al(p,\gamma)^{28}Si$ nuclear reaction profile	[144]
diopside (synthetic) $(CaMgSi_2O_6)$	// c-axis	Sr	1100-1250	2000	UB	607(+33)	2.940	-26.6	911	Thin film, sectioning, ion probe, Rutherford backscatter, anisotropy, pressure depend.	[149]
diopside $(Wo_{.99}En_{.99}Fs_{.02})$	// c-axis	^{85}Sr	1100-1300	0.1	UB/ N_2	406	-2.268	-22.0	710	Thin film, sectioning by grinding, scintillation counts	[149]
diopside (synthetic) $(CaMgSi_2O_6)$	// c-axis	Sm	1100-1250	0.1 to 2000	UB	590(+96)	2.146	-26.6	913	Thin film, sectioning, ion probe, Rutherford backscatter, anisotropy, pressure depend.	[149]
clinopyroxene $(Na_{.1}Ca_{.53}Mg_{1.1} Fe_{.17}Al_{.1}Si_{2.0}O_6)$	⊥ (001)	Ca-(Mg,Fe) interdiffusion	1150-1250	2500	UB/ GrPC	360.87 (±190)	-6.410	-24.0	801	Average D from lamellar homogenization experiments	[12]
wollastonite (synthetic? α-CaSiO₃)	sintered powder	^{45}Ca	900-1300?	0.006	UB	469	0.845	-22.0	721	Thin film, autoradiography profiles?	[110] [111]
åkermanite (syn) $(Ca_2MgSi_2O_7)$	// c-axis	^{18}O	1000-1300	0.1	CO_2	215 (±51)	-9.026	-19.5	483	Exchange with $C^{18}O_2$ atmosphere, ion probe profile	[165]
åkermanite (syn) $(Ca_2MgSi_2O_7)$	⊥ c-axis	^{18}O	800-1300	0.1	(CO)/ (CO_2)	278 (±33)	-6.328 (±1.282)	-19.9	555	Exchange with ^{18}O-enriched gass, ion probe profile	[143]
åkermanite (syn) $(Ca_2MgSi_2O_7)$	// c-axis	^{45}Ca	1100-1300	0.1	N_2	410	-0.301	-20.3	639	Thin film, sectioning by grinding, grindings counted	[127]
åkermanite (syn) $(Ca_2MgSi_2O_7)$	// c-axis	^{54}Mn	1100-1300	0.1	N_2	300	-4.569	-19.2	541	Thin film, sectioning by grinding, grindings counted	[127]
åkermanite (syn) $(Ca_2MgSi_2O_7)$	// c-axis	^{59}Fe	1100-1300	0.1	N_2	230	-7.377	-18.6	457	Thin film, sectioning by grinding, grindings counted	[127]
åkermanite (syn) $(Ca_2MgSi_2O_7)$	// c-axis	^{60}Co	1100-1300	0.1	N_2	230	-7.770	-19.0	474	Thin film, sectioning by grinding, grindings counted	[127]

Mineral, Glass, or Liquid	Orienta-tion	Diffusing Component	Temperature Range (°C)	P (MPa)	O_2 (MPa)	ΔE_a (kJ/mole)	log D_0 (or D) (m²/s)	log D 800°C	"T_c" (°C)	Experiment/Comments	Ref.
åkermanite (syn) ($Ca_2MgSi_2O_7$)	// c-axis	^{63}Ni	1100-1300	0.1	N_2	200	-8.301	-18.0	400	Thin film, sectioning by grinding, grindings counted	[127]
åkermanite (syn) ($Ca_2MgSi_2O_7$)	// c-axis	^{85}Sr	1100-1300	0.1	N_2	380	-1.745	-20.2	627	Thin film, sectioning by grinding, grindings counted	[127]
åkermanite (syn) ($Ca_2MgSi_2O_7$)	// c-axis	^{133}Ba	1100-1300	0.1	N_2	290	-4.854	-19.0	526	Thin film, sectioning by grinding, grindings counted	[127]
gehlenite (syn) ($Ca_2Al_2SiO_7$)	// c-axis	^{18}O	1000-1300	0.1	CO_2	186 (±16)	-11.361	-20.4	498	Exchange with $C^{18}O_2$ atmosphere, ion probe profile	[165]
gehlenite (syn) ($Ca_2Al_2SiO_7$)	// a-axis	^{18}O	1000-1300	0.1	CO_2	300 (±37)	-5.157	-19.8	566	Exchange with $C^{18}O_2$ atmosphere, ion probe profile	[165]
melilite (syn) ($Ak_{50}Gh_{50}$)	powder	^{18}O	799-1300	0.1	CO_2	140.2 (±0.4)	-9.066	-15.9	227	Exchange with $C^{18}O_2$, bulk analysis, spherical model	[84]
melilite (syn) ($Ak_{75}Gh_{25}$)	powder	^{18}O	799-1300	0.1	CO_2	133.5 (±0.4)	-9.143	-15.6	206	Exchange with $C^{18}O_2$, bulk analysis, spherical model	[84]
åkermanite - gehlenite couple	// c-axis	AlAl-MgSi interdiffusion	1200 1250	0.1	N_2		D=3.9x10^{-19} D=6.9x10^{-18}			EDXA profile of cross section, D = f(composition), maximum D reported here	[127]
epidote	powder	^2H	450-650	200 & 400	UB	57.7	-9.48	-12.3	-56	Enchange with ($^2H,^1H)_2O$, bulk analysis, "cylinder"	[70]
zoisite	powder	^2H	350-650	200 & 400	UB	102.5	-8.35	-13.3	79	Enchange with ($^2H,^1H)_2O$, bulk analysis, "cylinder"	[70]
olivine ($Fo_{91}Fa_9$)	// a-axis	"H"	800-1000	300 "wet"	IW	130 (±30)	-4.222 (±0.18)	-10.5	80	Exchange with water, IR step profiles of cross section slices	[118]
olivine ($Fo_{89.2}$)	powder	He "apparent diffusivity"	700-1400	0.0	UB	420 (±20)	1.1 (±0.7)	-19.3	610	Degassing experiment, spherical model, fractures!	[151]
olivine ($Fo_{≈92}Fa_{≈8}$)	// c-axis	^{18}O	1200-1400	0.1	IW & NO	266 (±11)	-9.585 + 0.21x log$_{10}$(f$_{O2}$) (f$_{O2}$ in Pa)	-22.5	691	Exchange with mixed $C^{18}O_2$ gas, $^{18}O(p,\alpha)^{15}N$ nuclear microanalysis profiles	[142]
olivine ($Fo_{≈90}Fa_{≈10}$)	// c-axis	^{18}O	1090-1500	0.1	10^{-12}-10^{-8}	318 (±17)	-5.174 + 0.34x log$_{10}$(P_{O2}) (P_{O2} in Pa)	-20.7	616	Exchange with mixed $H_2^{18}O$ gas, $^{18}O(p,\alpha)^{15}N$ nuclear microanalysis profiles	[61]
olivine ($Fo_{90}Fa_{10}$)	// a-axis & // c-axis	^{30}Si	1130-1530	0.1	10^{-5}-10^{-15}	291(±15)	-12.735(±0.18)- .19xln (P_{O2}/P_o)	-26.9	1047	Thin Fo film, Ruther-ford back-scattering profiles	[90]
olivine ($Fo_{90}Fa_{10}$)	// c-axis	Ca interdiffusion	1220-1350	0.1	10^{-9}	176	-9.155	-17.7	353	Cation exchange with basalt, microprobe profiles	[100]
olivine ($Fo_{90}Fa_{10}$)	// c-axis	Mn interdiffusion	1220-1350	0.1	10^{-9}	218	-7.167	-17.8	410	Cation exchange with basalt, microprobe profiles	[100]
olivine ($Fo_{90}Fa_{10}$)	// c-axis	Fe interdiffusion	1220-1350	0.1	10^{-9}	247	-8.000	-20.0	539	Cation exchange with basalt, microprobe profiles	[100]

Mineral, Glass, or Liquid	Orienta-tion	Diffusing Component	Temperature Range (°C)	P (MPa)	O_2 (MPa)	ΔE_a (kJ/mole)	log D_0 (or D) (m^2/s)	log D 800°C	"T_c" (°C)	Experiment/Comments	Ref.
olivine ($Fo_{90}Fa_{10}$-Fa_{100})	sintered powder	^{59}Fe	1130	0.1	10^{-10}-10^{-12}	n.d.	n.d.			log D_{59Fe} = -10.143 + 0.2 a_{O2} + 2.705 [Fe/(Fe+Mg)]	[85]
olivine ($Fo_{93.7}Fa_{6.3}$)	// c-axis	Ni	1149-1234	evac. tube	UB	193 (±10)	-8.959 (±0.36)	-18.4	404	Thin Ni film, microprobe profile, anisotropy found	[26]
olivine ($Fo_{92}Fa_8$)-fayalite powder	// c-axis (couple)	Fe-Mg interdiffusion	1125-1200	0.1	10^{-13}	243	-5.759	-17.6	432	Microprobe profile, D varies w/direction, composition, f_{O2}	[14]
olivine ($Fa_{97}Te_3$)-olivine ($Fo_{91}Fa_9$)	// c-axis (couple)	Fe-Mg interdiffusion	900-1100	evac. tube	UB	208.5(±18.8) +9.1 x [Mg/(Mg+Fe)]	D_0= 1.5(±0.3) x10^{-4}) - 1.1x [Mg/(Mg+Fe)]			Microprobe profile, D also varies with direction and P (ΔV_a=5.5x10^{-6}m^3/mole)	[124]
olivine(Mg_2SiO_4) - (Co_2SiO_4)	// c-axis (couple)	Co-Mg interdiffusion	1150-1300 1300-1400	0.1	air	196 526	-8.690 2.288	-18.2 -23.3	403 781	Microprobe profile, D's extrapolated to pure Fo	[125]
forsterite - liebensbergite	// c-axis (couple)	Ni-Mg interdiffusion	1200-1450	0.1	air	414 to 444	-1.652	-21.8	702	Microprobe profile, other interdiffusion coefficients	[126] [128]
grossularite ($Ca_{2.9}Fe_{.1}Al_{2.0}Si_{3.0}O_{12}$)	isotropic	^{18}O	1050 850	800 200	UB	n.d. n.d.	D=2.5x10^{-20} D=4.8x10^{-21}			Exchange with ^{18}O-enriched water, ion probe profiles	[58]
almandine ($Al_{67}Sp_{28}An_3Py_2$)	isotropic	^{18}O	800-1000	100	UB	301 (±46)	-8.222 (±0.740)	-22.9	725	Exchange with ^{18}O-enriched water, ion probe profiles	[31]
pyrope ($Py_{74}Al_{15}Gr_{10}Ur_1$)	isotropic	^{25}Mg	750-900	200	UB/ MH	239 (±16)	-8.009	-19.6	514	Thin ^{25}MgO film, ion probe profiles	[34]
$Alm_{80}Pyp_{20}$ - $Spess_{94}Alm_6$	isotropic (couple)	Fe	1300-1480	2900-4300	UB/ GrPC	275.43 (±36.49)	-7.194	-20.6	588	Calculated from interdiffusion experiments using model, (ΔV_a=5.6x10^{-6} m^3/mole)	[20]
$Alm_{80}Pyp_{20}$ - $Spess_{94}Alm_6$	isotropic (couple)	Mg	1300-1480	2900-4300	UB/ GrPC	284.52 (±37.55)	-6.959	-20.8	604	Calculated from interdiffusion experiments, (ΔV_a= 5.6(±2.9)x10^{-6} m^3/mole)	[20]
$Alm_{80}Pyp_{20}$ - $Spess_{94}Alm_6$	isotropic (couple)	Mn	1300-1480	2900-4300	UB/ GrPC	253.44 (±37.19)	-7.292	-19.6	526	Calculated from interdiffusion experiments, (ΔV_a= 5.3(±3.0)x10^{-6} m^3/mole)	[20]
almandine ($Al_{67}Sp_{28}An_3Py_2$)	isotropic	^{86}Sr	800-1000	100	UB	205 (±17)	-12.000(±0.602)	-22.0	616	Exchange with ^{86}Sr water solution, ion probe profiles	[31]
almandine ($Al_{67}Sp_{28}An_3Py_2$)	isotropic	^{145}Nd	800-1000	100	UB	184 (±29)	-12.523(±0.602)	-21.5	562	Exchange with ^{145}Nd water solution, ion probe profiles	[31]
pyrope	powder	^{151}Sm	1300-1500	3000	UB/ GrPC	140	-11.585	-18.4	321	Exchange with silicate melt, autoradiography, "sphere"	[80]
almandine ($Al_{67}Sp_{28}An_3Py_2$)	isotropic	^{167}Er	800-1000	100	UB	230 (±38)	-10.301(±0.763)	-21.5	605	Exchange with ^{167}Er water solution, ion probe profiles	[31]
$Alm_{80}Pyp_{20}$ - $Spess_{94}Alm_6$	isotropic (couple)	Fe-Mn interdiffusion	1300-1480	4000	UB/ GrPC	224.3 (±20.5)	-10.086	-21.0	571	Microprobe profiles, model fits of alm-rich composition	[41]

Mineral, Glass, or Liquid	Orienta-tion	Diffusing Component	Temperature Range (°C)	P (MPa)	O_2 (MPa)	ΔE_a (kJ/mole)	$\log D_0$ (or D) (m²/s)	$\log D$ 1200°C	"T_c" (°C)	Experiment/Comments	Ref.
titanite	// c-axis	^{18}O	700-900	100	UB/NO	301	-5.638	-20.3	591	Exchange with ^{18}O-enriched water, ion probe profiles	[129]
titanite	// c-axis	^{86}Sr	700-900	100	UB/NO	234	-9.420	-20.8	570	Exchange with ^{18}O-enriched water, ion probe profiles	[129]
titanite	// (100)	Pb	650-1027	0.1	air	328.5(±11.3)	-3.955(±0.315)	-19.9	591	Exchange with PbS powder, Rutherford backscattering	[22]
zircon	n.d.	Pb	550-800	0.1	air	142 (±8)	-11.699	-18.6	337	Ion implantation of Pb, Rutherford backscattering	[23]
rhyolite	glass	Li	297-909	0.1	air	92.1 (±1.3)	-5.599 (±0.079)	-8.9		Thin film of $LiNO_3$, ion probe profile on cross section	[92]
rhyolite (obsidian) Iceland	glass	^{24}Na	140-850	0.1	air	84.5 (±1.3)	-5.91 (±0.18)	-8.9		Thin film, serial sectioning by etching, counting surface	[91]
"haplogranite"	melt	"B-Si" interdiffusion	1200-1600	0.1	n.d.	288.5(±20.4)	-4.864 (±0.640)	-15.1		Ion probe profile of cross section	[18]
rhyolite(obsidian) Lake County, OR	melt	P	1200-1500	800	UB/GrPC	600.9(±11.7)	-12.652(±0.334)	-34.0		Apatite dissolution, microprobe profile, effect of water measured	[79]
rhyolite (obsidian) Lake County, OR	melt with 8% water	^{36}Cl	1100	1000	UB/GrPC		D=1.29x10^{-11}			Thin film of $Na^{36}Cl$, β-track profiles of cross section	[155]
rhyolite (obsidian) Iceland	glass	^{42}K	350-850	0.1	air	106.3 (±3.8)	-6.46 (±0.24)	-10.2		Thin film, serial sectioning by etching, counting surface	[91]
rhyolite (obsidian) Iceland	glass	Ca	630-930	0.1	air	283.7 (±4.6)	-0.69 (±0.22)	-10.7		Thin film, serial sectioning by etching, counting surface	[91]
rhyolite (obsidian) Iceland	glass	^{86}Rb	400-950	0.1	air	127.2 (±0.8)	-6.86 (±0.05)	-11.4		Thin film, serial sectioning by etching, counting surface	[91]
rhyolite (dehydrated) NM	glass	^{85}Sr	650-950	0.1	air	178.7 (±3.3)	-5.260 (±0.175)	-11.6		Thin film, serial sectioning by grinding, counting surface	[119]
rhyolite (obsidian) Lake County, OR	melt(dry)	Zr	1020-1500	800	UB/GrPC	408.8(±11.7)	-1.009 (±0.386)	-15.5		Zircon dissolution, microprobe profiles	[78]
rhyolite (obsidian) Lake County, OR	melt(wet)	Zr	1020-1385	800	UB/GrPC	197.9 (±8.0)	-5.523 (±0.301)	-12.5		Zircon dissolution, microprobe profiles	[78]
rhyolite (obsidian) Iceland	glass	^{134}Cs	600-920	0.1	air	208.4 (±8.4)	-5.04 (±0.44)	-12.4		Thin film, serial sectioning by etching, counting surface	[91]
rhyolite (dehydrated) NM	glass and melt	^{134}Cs	790-1300	0.1	air	201.3 (±12.1)	-6.01 (±0.45)	-13.1		Thin film, serial sectioning by etching, counting surface	[91]
rhyolite (obsidian) Lake County, OR	melt	^{134}Cs	700-800	210	UB/NO	81.68	-8.143	-11.0		Thin film, β-track profiles of cross section	[153]
rhyolite (dehydrated) NM	glass	^{133}Ba	650-950	0.1	air	188.7 (±6.3)	-5.42 (±0.30)	-12.1		Thin film, serial sectioning by grinding, counting surface	[119]

Mineral, Glass, or Liquid	Orienta-tion	Diffusing Component	Temperature Range (°C)	P (MPa)	O_2 (MPa)	ΔE_a (kJ/mole)	log D_0 (or D) (m^2/s)	log D 1200°C	"Tc" (°C)	Experiment/Comments	Ref.
rhyolite (dehydrated) NM	glass and melt	Ce	875-1100	0.1	air	490.4 (±23.9)	2.72 (±0.99)	-14.7		Thin film, serial sectioning by etching, counting surface	[91]
rhyolite (dehydrated) NM	glass and melt	Eu	700-1050	0.1	air	288.7 (±5.0)	-3.11 (0.22)	-13.3		Thin film, serial sectioning by etching, counting surface	[91]
rhyolite (obsidian) Lake County, OR	melt 6% water	LREE	1000-1400	800	UB/ GrPC	251.5(±42.3)	-4.638 (±1.436)	-13.6		Monazite dissolution, microprobe profiles	[138]
rhyolite (obsidian) Lake County, OR	melt 1% water	LREE	1000-1400	800	UB/ GrPC	510.9(±59.0)	3.362 (±0.629)	-14.8		Monazite dissolution, microprobe profiles	[138]
rhyolite (obsidian) Mono Craters	glass	H_2O	400-850	0.1	N_2	103 (±5)	-14.59 (±1.59)	-18.2		Dehydration in N_2, FTIR profile, equilibrium model	[166]
rhyolite (obsidian) New Mexico	glass	H_2O	510-980	0.1	air	46.48 (±11.40)	-10.90 (±0.56)	-12.5		Dehydration in air, bulk weight loss, low water	[93]
rhyolite (obsidian) Lake County, OR	melt with 8% water	$^{14}CO_2$	800-1100	1000	UB/ GrPC	75 (±21)	-7.187	-9.9		Thin film of $Na_2\,^{14}CO_3$, β-track profiles of cross section	[155]
basalt (alkali)	melt	^{6}Li	1300-1400	0.1	air	115.5	-5.125	-9.2		Thin film of ^{6}LiCl, ion probe profile of cross section	[116]
basalt Goose Island	melt	O	1160-1360	0.1	IW to CO_2	215.9 (±13.4)	-2.439	-10.1		Oxidation/reduction of bead, thermo-gravimetric balance	[160]
basalt (alkali olivine) BC	melt	O	1280-1400	400	UB/ GrPC	293 (±29)	-0.790 (±2.51)	-11.2		Reduction by graphite, bulk FeO analysis by titration	[40]
basalt (alkali olivine) BC	melt	O	1280-1450	1200	UB/ GrPC	360 (±25)	1.450 (±0.081)	-11.3		Reduction by graphite, bulk FeO analysis by titration	[40]
basalt (alkali olivine) BC	melt	O	1350-1450	2000	UB/ GrPC	297 (±59)	-0.770 (±1.87)	-11.3		Reduction by graphite, bulk FeO analysis by titration	[40]
basalt (tholeiite) 1921 Kilauea	melt	O	1300-1450	1200	UB/ GrPC	213 (±17)	-3.010 (±0.59)	-10.6		Reduction by graphite, bulk FeO analysis by titration	[40]
basalt (FeTi) Galapagos	melt	^{18}O	1320-1500	0.1	CO_2 & O_2	251 (±29)	-2.854	-11.8		Exchange with ^{18}O-selected gas, bulk analysis of sphere	[15]
"basalt" (Fe-free) (synthetic)	melt	Ar	1300-1450	1000-3000		113.2 (±7.5)	-6.140 (±0.068)	-10.2		Method not described	[39]
basalt ("alkali") Tenerife	melt	^{24}Na	1300-1400	0.1	air	163 (±13)	-4.02 (±0.46)	-9.8		Thin film, serial sectioning by grinding, counting surface	[116]
basalt (tholeiite) 1921 Kilauea	melt	^{45}Ca	1260-1440	0.1	air	184.1	-4.272	-10.8		Thin film, β-track profiles of cross-section on film	[89]
"basalt" (Fe-free) (synthetic)	melt	^{45}Ca	1100-1400	0.1	UB	106.3	-6.301	-10.1		Thin film of $^{45}CaCl$, β-track profiles of cross section	[152]
"basalt" (Fe-free) (synthetic)	melt	^{45}Ca	1100-1400	1000	UB	141.0	-5.284	-10.3		Thin film of $^{45}CaCl$, β-track profiles of cross section	[152]
"basalt" (Fe-free) (synthetic)	melt	^{45}Ca	1100-1400	2000	UB	208.4	-3.211	-10.6		Thin film of $^{45}CaCl$, β-track profiles of cross section	[152]

Mineral, Glass, or Liquid	Orienta-tion	Diffusing Component	Temperature Range (°C)	P (MPa)	O_2 (MPa)	ΔE_a (kJ/mole)	$\log D_0$ (or D) (m^2/s)	$\log D$ 1200°C	"T_c" (°C)	Experiment/Comments	Ref.
basalt ("alkali") Tenerife	melt	[46]Sc	1300-1400	0.1	air	197 (±8)	-4.55 (±0.31)	-11.5		Thin film, serial sectioning by grinding, counting surface	[116]
basalt ("alkali") Tenerife	melt	[54]Mn	1300-1400	0.1	air	201 (±25)	-3.80 (±0.81)	-10.9		Thin film, serial sectioning by grinding, counting surface	[116]
basalt ("alkali") Tenerife	melt	[59]Fe	1300-1400	0.1	air	264 (±17)	-2.20 (±0.59)	-11.5		Thin film, serial sectioning by grinding, counting surface	[116]
basalt (tholeiite) 1921 Kilauea	melt	[60]Co	1260-1440	0.1	air	151.9	-5.276	-10.7		Thin film, serial sectioning by grinding, counting surface	[89]
basalt ("alkali") Tenerife	melt	[60]Co	1300-1400	0.1	air	201 (±21)	-3.83 (±0.61)	-11.0		Thin film, serial sectioning by grinding, counting surface	[116]
basalt (tholeiite) 1921 Kilauea	melt	[85]Sr	1260-1440	0.1	air	182.0	-4.556	-11.0		Thin film, serial sectioning by grinding, counting surface	[89]
basalt ("alkali") Tenerife	melt	[85]Sr	1300-1400	0.1	air	213 (±25)	-3.46 (±0.83)	-11.0		Thin film, serial sectioning by grinding, counting surface	[116]
basalt (tholeiite) 1921 Kilauea	melt	[133]Ba	1260-1440	0.1	air	164.9	-5.229	-11.1		Thin film, serial sectioning by grinding, counting surface	[89]
basalt ("alkali") Tenerife	melt	[133]Ba	1300-1400	0.1	air	172 (±17)	-5.00 (±0.54)	-11.1		Thin film, serial sectioning by grinding, counting surface	[116]
basalt ("alkali") Tenerife	melt	[134]Cs	1300-1400	0.1	air	272 (±17)	-2.00 (±0.60)	-11.6		Thin film, serial sectioning by grinding, counting surface	[116]
basalt (tholeiite) 1921 Kilauea	melt	[152]Eu, [153]Gd	1320-1440 1320-1210	0.1	air	169.9	-5.237 D=1.4x10^{-11}			Thin film, serial sectioning by grinding, counting surface	[120]
"basalt" (Fe-free) (synthetic)	melt	[14]CO_2	1350-1500	1500	UB/ GrPC	195.0	-3.449	-10.4		Thin film of $Na^{14}CO_3$, β-track profiles of cross section, pressure dependence	[159]

Key to oxygen fugacity or atmosphere abbreviations in data table

CO_2 -   Pure carbon dioxide atmosphere
GM -   Graphite-methane buffer
IW -   Iron-wustite buffer
MH -   Magnetite-hematite buffer
N_2 -   Pure nitrogen atmosphere
NO -   Nickel-nickel oxide
O_2 -   Pure oxygen atmosphere
QFM -   Quartz-fayalite-magnetite buffer
UB -   Unbuffered oxygen fugacity
UB/GrPC -   Unbuffered, but f_{O2} limited by the graphite-bearing piston-cylinder assembly
UB/NO -   Unbuffered, but near nickel-nickel oxide due to the cold seal pressure vessel

REFERENCES

1. Ashworth, J. R., Birdi, J. J., and Emmett, T. F., Diffusion in coronas around clinopyroxene: modelling with local equilibrium and steady state, and a non-steady-state modification to account for zoned actinolite-hornblende, *Contrib. Mineral. Petrol.*, *109*, 307-325, 1992.

2. Askill, J., *Tracer Diffusion Data for Metals, Alloys, and Simple Oxides*, 97 pp., Plenum Press, New York, 1970.

3. Baker, D. R., Interdiffusion of hydrous dacitic and rhyolitic melts and the efficacy of rhyolite contamination of dacitic enclaves, *Contrib. Mineral. Petrol.*, *106*, 462-473, 1991.

4. Baker, D. R., The effect of F and Cl on the interdiffusion of peralkaline intermediate and silicic melts, *Am. Mineral.*, *78*, 316-324, 1993.

5. Barrer, R. M., Bartholomew, R. F., and Rees, L. V. C., Ion exchange in porous crystals. Part II. The relationship between self- and exchange-diffusion coefficients, *J. Phys. Chem. Solids*, *24*, 309-317, 1963.

6. Barrer, Richard M., *Diffusion in and through Solids*, 464 pp., Cambridge University Press, Cambridge, England, 1951.

7. Besancon, J. R., Rate of disordering in orthopyroxenes, *Am. Mineral.*, *66*, 965-973, 1981.

8. Boltzmann, L., Zur Integration der Diffusionsgleichung bei variabeln Diffusion-coefficienten *Ann. Physik Chem.*, *53*, 959-964, 1894.

9. Brabander, D. J., and Giletti, B. J., Strontium diffusion kinetics in amphiboles (abstract), *AGU 1992 Fall Meeting*, supplement to *Eos Trans. AGU*, *73*, 641, 1992.

10. Brady, J. B., Reference frames and diffusion coefficients, *Am. J. Sci.*, *275*, 954-983, 1975.

11. Brady, J. B., Intergranular diffusion in metamorphic rocks, *Am. J. Sci.*, *283-A*, 181-200, 1983.

12. Brady, J. B., and McCallister, R. H., Diffusion data for clinopyroxenes from homogenization and self-diffusion experiments, *Am. Mineral.*, *68*, 95-105, 1983.

13. Brenan, J. M., Diffusion of chlorine in fluid-bearing quartzite: Effects of fluid composition and total porosity, *Contrib. Mineral. Petrol.*, *115*, 215-224, 1993.

14. Buening, D. K., and Buseck, P. R., Fe-Mg lattice diffusion in olivine, *J. Geophys. Res.*, *78*, 6852-6862, 1973.

15. Canil, D., and Muehlenbachs, K., Oxygen diffusion in an Fe-rich basalt melt, *Geochim. Cosmochim. Acta*, *54*, 2947-2951, 1990.

16. Carlson, W. D., and Johnson, C. D., Coronal reaction textures in garnet amphibolites of the Llano Uplift, *Am. Mineral.*, *76*, 756-772, 1991.

17. Carslaw, H. S., Jaeger, J. C., *Conduction of Heat in Solids*, 510 pp., Oxford, Clarendon Press, 1959.

18. Chakraborty, S., Dingwell, D., and Chaussidon, M., Chemical diffusivity of boron in melts of haplogranitic composition, *Geochim. Cosmochim. Acta*, *57*, 1741-1751, 1993.

19. Chakraborty, S., and Ganguly, J., Compositional zoning and cation diffusion in garnets, in *Diffusion, Atomic Ordering, and Mass Transport*, edited by Ganguly, J., pp. 120-175, Springer-Verlag, New York,

1991.

20. Chakraborty, S., and Ganguly, J., Cation diffusion in aluminosilicate garnets: experimental determination in spessartine-almandine diffusion couples, evaluation of effective binary diffusion coefficients, and applications, *Contrib. Mineral. Petrol.*, *111*, 74-86, 1992.

21. Cherniak, D. J., Diffusion of Pb in feldspar measured by Rutherford backscatteing spectroscopy, *AGU 1992 Fall Meeting*, supplement to *Eos Trans. AGU*, *73*, 641, 1992.

22. Cherniak, D., Lead diffusion in titanite and preliminary results on the effects of radiation damage on Pb transport, *Chem. Geol.*, *110*, 177-194, 1993.

23. Cherniak, D. J., Lanford, W. A., and Ryerson, R. J., Lead diffusion in apatite and zircon using ion implantation and Rutherford backscattering techniques, *Geochim. Cosmochim. Acta*, *55*, 1663-1673, 1991.

24. Cherniak, D. J., and Watson, E. B., A study of strontium diffusion in K-feldspar, Na-K feldspar and anorthite using Rutherford backscattering spectroscopy, *Earth Planet. Sci. Lett.*, *113*, 411-425, 1992.

25. Christoffersen, R., Yund, R. A., and Tullis, J., Interdiffusion of K and Na in alkali feldspars, *Am. Mineral.*, *68*, 1126-1133, 1983.

26. Clark, A. M., and Long, J. V. P., The anisotropic diffusion of nickel in olivine, in *Thomas Graham Memorial Symposium on Diffusion Processes*, edited by Sherwood, J. N., Chadwick, A. V., Muir, W. M., and Swinton, F. L., pp. 511-521, Gordon and Breach, New York, 1971.

27. Connolly, C., and Muehlenbachs, K., Contrasting oxygen diffusion in nepheline, diopside and other silicates and their relevance to isotopic systematics in meteorites, *Geochim. Cosmochim. Acta, 52*, 1585-1591, 1988.

28. Cooper, A. R., The use and limitations of the concept of an effective binary diffusion coefficient for multi-component diffusion, in *Mass Transport in Oxides*, edited by Wachtman, J. B., Jr., and Franklin, A. D., pp. 79-84, National Bureau of Standards, Washington, 1968.

29. Cooper, A. R., Jr. Vector space treatment of multicomponent diffusion, in *Geochemical Transport and Kinetics*, edited by Hofmann, A. W., Giletti, B. J., Yoder, H. S., Jr., and Yund, R. A., pp. 15-30, Carnegie Institution of Washington, Washington, 1974.

30. Cooper, A. R., and Varshneya, A. K., Diffusion in the system K_2O-SrO-SiO_2, effective binary diffusion coefficients, *Am. Ceram. Soc. J., 51*, 103-106, 1968.

31. Coughlan, R. A. N., Studies in diffusional transport: grain boundary transport of oxygen in feldspars, strontium and the REE's in garnet, and thermal histories of granitic intrusions in south-central Maine using oxygen isotopes, Ph.D. thesis, Brown University, Providence, Rhode Island, 1990.

32. Crank, J., *The Mathematics of Diffusion*, 414 pp., Clarendon Press, Oxford, 1975.

33. Cullinan, H. T. , Jr., Analysis of the flux equations of multi-component diffusion, *Ind. Engr. Chem. Fund., 4*, 133-139, 1965.

34. Cygan, R. T., and Lasaga, A.

C., Self-diffusion of magnesium in garnet at 750-900°C, *Am. J. Sci., 285*, 328-350, 1985.

35. Darken, L. S., Diffusion, mobility and their interrelation through free energy in binary metallic systems, *Am. Inst. Min. Metal. Engrs. Trans., 175*, 184-201, 1948.

36. de Groot, S. R., Mazur, P., *Non-equilibrium Thermodynamics*, 510 pp., North Holland, Amsterdam, 1962.

37. Dennis, P. F., Oxygen self-diffusion in quartz under hydrothermal conditions, *J. Geophys. Res., 89*, 4047-4057, 1984.

38. Dodson, M. H., Closure temperature in cooling geochronological and petrological problems, *Contrib. Mineral. Petrol., 40*, 259-274, 1973.

39. Draper, D. S., and Carroll, M. R., Diffusivity of Ar in haplobasaltic liquid at 10 to 30 kbar (abstract), *AGU 1992 Fall Meeting*, supplement to *Eos Trans. AGU, 73*, 642, 1992.

40. Dunn, T., Oxygen chemical diffusion in three basaltic liquids at elevated temperatures and pressures, *Geochim. Cosmochim. Acta, 47*, 1923-1930, 1983.

41. Elphick, S. C., Ganguly, J., and Loomis, T. P., Experimental determination of cation diffusivities in aluminosilicate garnets, I. Experimental methods and interdiffusion data, *Contrib. Mineral. Petrol., 90*, 36-44, 1985.

42. Elphick, S. C., Graham, C. M., and Dennis, P. F., An ion microprobe study of anhydrous oxygen diffusion in anorthite: a comparison with hydrothermal data and some geological implications, *Contrib. Mineral. Petrol., 100*, 490-495, 1988.

43. Farver, J. R., Oxygen self-

diffusion in diopside with application to cooling rate determinations, *Earth Planet. Sci. Lett., 92*, 386-396, 1989.

44. Farver, J. R., and Giletti, B. J., Oxygen diffusion in amphiboles, *Geochim. Cosmochim. Acta, 49*, 1403-1411, 1985.

45. Farver, J. R., and Giletti, B. J., Oxygen and strontium diffusion kinetics in apatite and potential applications to thermal history determinations, *Geochim. Cosmochim. Acta, 53*, 1621-1631, 1989.

46. Farver, J. R., and Yund, R. A., The effect of hydrogen, oxygen, and water fugacity on oxygen diffusion in alkali feldspar, *Geochim. Cosmochim. Acta, 54*, 2953-2964, 1990.

47. Farver, J. R., and Yund, R. A., Measurement of oxygen grain boundary diffusion in natural, fine-grained quartz aggregates, *Geochim. Cosmochim. Acta, 55*, 1597-1607, 1991a.

48. Farver, J. R., and Yund, R. A., Oxygen diffusion in quartz: Dependence on temperature and water fugacity, *Chem. Geol., 90*, 55-70, 1991b.

49. Farver, J. R., and Yund, R. A., Oxygen diffusion in a fine-grained quartz aggregate with wetted and nonwetted microstructures, *J. Geophys. Res., 97*, 14017-14029, 1992.

50. Fick, A., Über diffusion, *Ann. Physik Chem., 94*, 59, 1855.

51. Fisher, G. W., Nonequilibrium thermodynamics as a model for diffusion-controlled metamorphic processes, *Am. J. Sci., 273*, 897-924, 1973.

52. Foland, K. A., ^{40}Ar diffusion in homogeneous orthoclase and an interpretation of Ar diffusion in K-feldspars, *Geochim. Cosmochim. Acta, 38*, 151-166, 1974a.

53. Foland, K. A., Alkali diffusion in orthoclase, in *Geochemical Transport and Kinetics*, edited by Hofmann, A. W., Giletti, B. J., Yoder, H. S., Jr., and Yund, R. A., pp. 77-98, Carnegie Institution of Washington, Washington, 1974b.

54. Fortier, S. M., and Giletti, B. J., Volume self-diffusion of oxygen in biotite, muscovite, and phlogopite micas, *Geochim. Cosmochim. Acta, 55*, 1319-1330, 1991.

55. Foster, C. T., A thermodynamic model of mineral segregations in the lower sillimanite zone near Rangeley, Maine, *Am. Mineral., 66*, 260-277, 1981.

56. Freer, R., Self-diffusion and impurity diffusion in oxides, *J. Materials Sci., 15*, 803-824, 1980.

57. Freer, R., Diffusion in silicate minerals and glasses: a data digest and guide to the literature, *Contrib. Mineral. Petrol., 76*, 440-454, 1981.

58. Freer, R., and Dennis, P. F., Oxygen diffusion studies. I. A preliminary ion microprobe investigation of oxygen diffusion in some rock-forming minerals, *Mineral. Mag., 45*, 179-192, 1982.

59. Freer, R., and Hauptman, Z., An experimental study of magnetite-titanomagnetite interdiffusion, *Phys. Earth Planet. Inter., 16*, 223-231, 1978.

60. Ganguly, J., and Tazzoli, V., Fe^{+2}-Mg interdiffusion in orthopyroxene: constraints from cation ordering and structural data and implications for cooling rates of meteorites (abstract), in *Lunar and Planet. Science XXIV*, pp. 517-518, Lunar and Planet. Institute, Houston, 1992.

61. Gérard, O., and Jaoul, O.,

Oxygen diffusion in San Carlos olivine, *J. Geophys. Res., 94*, 4119-4128, 1989.

62. Giletti, B. J., Studies in diffusion I: argon in phlogopite mica, in *Geochemical Transport and Kinetics*, edited by Hofmann, A. W., Giletti, B. J., Yoder, H. S., Jr., and Yund, R. A., pp. 107-115, Carnegie Institution of Washington, Washington, 1974.

63. Giletti, B. J., Rb and Sr diffusion in alkali feldspars, with implications for cooling histories of rocks, *Geochim. Cosmochim. Acta, 55*, 1331-1343, 1991.

64. Giletti, B. J., Diffusion kinetics of Sr in plagioclase (abstract), *AGU 1992 Spring Meeting*, supplement to *Eos Trans. AGU, 73*, 373, 1992.

65. Giletti, B. J., and Hess, K. C., Oxygen diffusion in magnetite, *Earth Planet. Sci. Lett., 89*, 115-122, 1988.

66. Giletti, B. J., Semet, M. P., and Yund, R. A., Studies in diffusion -- III. Oxygen in feldspars: an ion microprobe determination, *Geochim. Cosmochim. Acta, 42*, 45-57, 1978.

67. Giletti, B. J., and Tullis, J., Studies in diffusion. IV. Pressure dependence of Ar Diffusion in Phlogopite mica, *Earth Planet. Sci. Lett., 35*, 180-183, 1977.

68. Giletti, B. J., and Yund, R. A., Oxygen diffusion in quartz, *J. Geophys. Res., 89*, 4039-4046, 1984.

69. Giletti, B. J., Yund, R. A., and Semet, M., Silicon diffusion in quartz, *Geol. Soc. Am. Abstr. Prog., 8*, 883-884, 1976.

70. Graham, C. M., Experimental hydrogen isotope studies III: diffusion of hydrogen in hydrous

minerals, and stable isotope exchange in metamorphic rocks, *Contrib. Mineral. Petrol., 76*, 216-228, 1981.

71. Graham, C. M., and Elphick, S. C., Some experimental constraints on the role of hydrogen in oxygen and hydrogen diffusion and Al-Si interdiffusion in silicates, in *Diffusion, Atomic Ordering, and Mass Transport: Selected Problems in Geochemistry*, edited by Ganguly, J., pp. 248-285, Springer-Verlag, New York, 1991.

72. Graham, C. M., Viglino, J. A., and Harmon, R. S., Experimental study of hydrogen-isotope exchange between aluminous chlorite and water and of hydrogen diffusion in chlorite, *Am. Mineral., 72*, 566-579, 1987.

73. Griggs, D. T., Hydrolytic weakening of quartz and other silicates, *Geophys. J., 14*, 19-31, 1967.

74. Grove, T. L., Baker, M. B., and Kinzler, R. J., Coupled CaAl-NaSi diffusion in plagioclase feldspar: experiments and applications to cooling rate speedometry, *Geochim. Cosmochim. Acta, 48*, 2113-2121, 1984.

75. Gupta, P. K., and Cooper, A. R., Jr., The [D] matrix for multicomponent diffusion, *Physica, 54*, 39-59, 1971.

76. Harrison, T. M., Diffusion of ^{40}Ar in hornblende, *Contrib. Mineral. Petrol., 78*, 324-331, 1981.

77. Harrison, T. M., Duncan, I., and McDougall, I., Diffusion of ^{40}Ar in biotite: temperature, pressure and compositional effects, *Geochim. Cosmochim. Acta, 49*, 2461-2468, 1985.

78. Harrison, T. M., and Watson,

E. B., Kinetics of zircon dissolution and zirconium diffusion in granitic melts of variable water content, *Contrib. Mineral. Petrol.*, *84*, 66-72, 1983.

79. Harrison, T. M., and Watson, E. B., The behavior of apatite during crustal anatexis: equilibrium and kinetic considerations, *Geochim. Cosmochim. Acta*, *48*, 1467-1477, 1984.

80. Harrison, W. J., and Wood, B. J., An experimental investigation of the partitioning of REE between garnet and liquid with reference to the role of defect equilibria, *Contrib. Mineral. Petrol.*, *72*, 145-155, 1980.

81. Harrop, P. J., Self-diffusion in simple oxides (a bibliography), *J. Materials Sci.*, *3*, 206-222, 1968.

82. Hart, S. R., Diffusion compensation in natural silicates, *Geochim. Cosmochim. Acta*, *45*, 279-291, 1981.

83. Hartley, G. S., and Crank, J., Some fundamental definitions and concepts in diffusion processes, *Trans. Faraday Soc.*, *45*, 801-818, 1949.

84. Hayashi, T., and Muehlenbachs, K., Rapid oxygen diffusion in melilite and its relevance to meteorites, *Geochim. Cosmochim. Acta*, *50*, 585-591, 1986.

85. Hermeling, J., and Schmalzreid, H., Tracerdiffusion of the Fe-cations in Olivine $(Fe_xMg_{1-x})_2$ SiO_4 (III), *Phys. Chem. Miner.*, *11*, 161-166, 1984.

86. Hofmann, A. W., Diffusion in natural silicate melts: a critical review, in *Physics of Magmatic Processes*, edited by Hargraves, R. B., pp. 385-417, Princeton Univ. Press, 1980.

87. Hofmann, A. W., and Giletti,

B. J., Diffusion of geochronologically important nuclides in minerals under hydrothermal conditions, *Eclogae Geol. Helv.*, *63*, 141-150., 1970.

88. Hofmann, A. W., Giletti, B. J., Hinthorne, J. R., Andersen, C. A., and Comaford, D., Ion microprobe analysis of a potassium self-diffusion experiment in biotite, *Earth Planet. Sci. Lett.*, *24*, 48-52, 1974.

89. Hofmann, A. W., and Magaritz, M., Diffusion of Ca, Sr, Ba, and Co in a basalt melt, *J. Geophys. Res.*, *82*, 5432-5440, 1977.

90. Houlier, B., Cheraghmakani, M., and Jaoul, O., Silicon diffusion in San Carlos olivine, *Phys. Earth Planet. Inter.*, *62*, 329-340, 1990.

91. Jambon, A., Tracer diffusion in granitic melts, *J. Geophys. Res.*, *87*, 10797-10810, 1982.

92. Jambon, A., and Semet, M. P., Lithium diffusion in silicate glasses of albite, orthoclase, and obsidian composition: an ion-microprobe determination, *Earth Planet. Sci. Lett.*, *37*, 445-450, 1978.

93. Jambon, A., Zhang, Y., and Stolper, E. M., Experimental dehydration of natural obsidian and estimation of D_{H2O} at low water contents, *Geochim. Cosmochim. Acta*, *56*, 2931-2935, 1992.

94. Joesten, R., Evolution of mineral assemblage zoning in diffusion metasomatism, *Geochim. Cosmochim. Acta*, *41*, 649-670, 1977.

95. Joesten, R., Grain-boundary diffusion kinetics in silicates and oxide minerals, in *Diffusion, Atomic Ordering, and Mass Transport: Selected Problems in Geochemistry*, edited by Ganguly, J., pp. 345-

395, Springer-Verlag, New York, 1991a.

96. Joesten, R., Local equilibrium in metasomatic processes revisited. Diffusion-controlled growth of chert nodule reaction rims in dolomite, *Am. Mineral.*, *76*, 743-755, 1991b.

97. Joesten, R., and Fisher, G., Kinetics of diffusion-controlled mineral growth in the Christmas Mountains (Texas) contact aureole, *Geol. Soc. Am. Bull.*, *100*, 714-732, 1988.

98. Johnson, C. D., and Carlson, W. D., The origin of olivine-plagioclase coronas in meta-gabbros from the Adirondack Mountains, New York, *J. Metamorph. Geol.*, *8*, 697-717, 1990.

99. Jost, W., *Diffusion in Solids, Liquids, and Gases*, 558 pp., Academic Press, New York, 1960.

100. Jurewicz, A. J. G., and Watson, E. B., Cations in olivine, part 2: diffusion in olivine xenocrysts, with applications to petrology and mineral physics, *Contrib. Mineral. Petrol.*, *99*, 186-201, 1988.

101. Kasper, R. B., Cation and oxygen diffusion in albite, Ph.D. thesis, Brown University, Providence, Rhode Island, 1975.

102. Kingery, W. D., Plausible concepts necessary and sufficient for interpretation of grain boundary phenomena: I, grain boundary characteristics, structure, and electrostatic potential, *Am. Ceram. Soc. J.*, *57*, 1-8, 1974a.

103. Kingery, W. D., Plausible concepts necessary and sufficient for interpretation of grain boundary phenomena: II, solute segregation, grain boundary diffusion, and general discussion, *Am. Ceram. Soc. J.*, *57*, 74-83, 1974b.

104. Kronenberg, A. K., Kirby, S. H., Aines, R. D., and Rossman, G. R., Solubility and diffusional uptake of hydrogen in quartz at high water pressures: implications for hydrolytic weakening, *J. Geophys. Res.*, *91*, 12723-12744, 1986.

105. Lasaga, A. C., Multicomponent exchange and diffusion in silicates, *Geochim. Cosmochim. Acta*, *43*, 455-469, 1979.

106. Lasaga, A. C., The atomistic basis of diffusion: defects in minerals, in *Kinetics of Geochemical Processes*, edited by Lasaga, A. C., and Kirkpatrick, R. J., pp. 261-320, Mineralogical Society of America, Washington, 1981.

107. Lasaga, A. C., Geospeedometry: an extension of geothermometry, in *Kinetics and Equilibrium in Mineral Reactions*, edited by Saxena, S. K., pp. 81-114, Springer-Verlag, New York, 1983.

108. Lesher, C. E., and Walker, D., Thermal diffusion in petrology, in *Diffusion, Atomic Ordering, and Mass Transport: Selected Problems in Geochemistry*, edited by Ganguly, J., pp. 396-451, Springer-Verlag, New York, 1991.

109. Lin, T. H., and Yund, R. A., Potassium and sodium self-diffusion in alkali feldspar, *Contrib. Mineral. Petrol.*, *34*, 177-184, 1972.

110. Lindner, R., Studies on solid state reactions with radiotracers, *J. Chem. Phys.*, *23*, 410-411, 1955.

111. Lindner, R., Silikatbildung durch Reaktion im festen Zustand, *Z. Physik. Chem.*, *6*, 129-142, 1956.

112. Lindström, R., Chemical diffusion in alkali halides, *J. Phys. Chem. Solids*, *30*, 401-

405, 1969.

113. Lindström, R., Chemical interdiffusion in binary ionic solid solutions and metal alloys with changes in volume, *J. Phys. C: Solid State*, *7*, 3909-3929, 1974.

114. Liu, M., and Yund, R. A., NaSi-CaAl interdiffusion in plagioclase, *Am. Mineral.*, *77*, 275-283, 1992.

115. Loomis, T. P., Ganguly, J., and Elphick, S. C., Experimental determination of cation diffusivities in aluminosilicate garnets II. Multicomponent simulation and tracer diffusion coefficients, *Contrib. Mineral. Petrol.*, *90*, 45-51, 1985.

116. Lowry, R. K., Henderson, P., and Nolan, J., Tracer diffusion of some alkali, alkaline-earth and transition element ions in a basaltic and an andesitic melt, and the implications concerning melt structure, *Contrib. Mineral. Petrol.*, *80*, 254-261, 1982.

117. Lowry, R. K., Reed, S. J. B., Nolan, J., Henderson, P., and Long, J. V. P., Lithium tracer-diffusion in an alkali-basalt melt -- an ion-microprobe determination, *Earth Planet. Sci. Lett.*, *53*, 36-41, 1981.

118. Mackwell, S. J., and Kohlstedt, D. L., Diffusion of hydrogen in olivine: implications for water in the mantle, *J. Geophys. Res.*, *95*, 5079-5088, 1990.

119. Magaritz, M., and Hofmann, A. W., Diffusion of Sr, Ba, and Na in obsidian, *Geochim. Cosmochim. Acta*, *42*, 595-605, 1978a.

120. Magaritz, M., and Hofmann, A. W., Diffusion of Eu and Gd in basalt and obsidian, *Geochim. Cosmochim. Acta*, *42*, 847-858, 1978b.

121. Manning, J. R., *Diffusion*

Kinetics for Atoms in Crystals, 257 pp., Van Nostrand, Princeton, 1968.

122. Matano, C., On the relation between the diffusion coefficients and concentrations of solid metals, *Japan J. Phys.*, *8*, 109-113, 1933.

123. McDougall, I., Harrison, T. M., *Geochronology and Thermochronology by the* $^{40}Ar/^{39}Ar$ *Method*, 212 pp., Oxford Univ. Press, New York, 1988.

124. Meisner, D. J., Cationic diffusion in olivine to 1400°C and 35 kbar, in *Geochemical Transport and Kinetics*, edited by Hofmann, A. W., Giletti, B. J., Yoder, H. S., Jr., and Yund, R. A., pp. 117-129, Carnegie Institution of Washington, Washington, 1974.

125. Morioka, M., Cation diffusion in olivine -- I. Cobalt and magnesium, *Geochim. Cosmochim. Acta*, *44*, 759-762, 1980.

126. Morioka, M., Cation diffusion in olivine -- II. Ni-Mg, Mn-Mg, Mg and Ca, *Geochim. Cosmochim. Acta*, *45*, 1573-1580, 1981.

127. Morioka, M., and Nagasawa, H., Diffusion in single crystals of melilite: II. Cations, *Geochim. Cosmochim. Acta*, *55*, 751-759, 1991a.

128. Morioka, M., and Nagasawa, H., Ionic diffusion in olivine, in *Diffusion, Atomic Ordering, and Mass Transport: Selected Problems in Geochemistry*, edited by Ganguly, J., pp. 176-197, Springer-Verlag, New York, 1991b.

129. Morishita, Y., Giletti, B. J., and Farver, J. R., Strontium and oxygen self-diffusion in titanite (abstract), *Eos Trans. AGU*, *71*, 652, 1990.

130. Muehlenbachs, K., and Connolly, C., Oxygen diffusion

in leucite, in *Stable Isotope Geochemistry: A Tribute to Samuel Epstein,* edited by Taylor, H. P., Jr., O'Neil, J. R., and Kaplan, I. R., pp. 27-34, The Geochemical Society, San Antonio, Texas, 1991.

131. Nye, J. F., *Physical Properties of Crystals,* 322 pp., Clarendon Press, Oxford, 1957.

132. Onsager, L., Reciprocal relations in irreversible processes, I, *Physical Rev., 37,* 405-426, 1931a.

133. Onsager, L., Reciprocal relations in irreversible processes II, *Physical Rev., 38,* 2265-2279, 1931b.

134. Onsager, L., Theories and problems of liquid diffusion, *Ann. N.Y. Acad. Sci., 46,* 241-265, 1945.

135. Philibert, Jean, *Atom Movements: Diffusion and Mass Transport in Solids,* 577 pp., Editions de Physique, Les Ulis, France, 1991.

136. Price, G. D., Diffusion in the titanomagnetite solid solution, *Mineral. Mag., 44,* 195-200, 1981.

137. Prigogine, I., *Introduction to Thermodynamics of Irreversible Processes,* 147 pp., Wiley Interscience, New York, 1967.

138. Rapp, R. A., and Watson, E. B., Monazite solubility an dissolution kinetics: implications for the thorium and light rare earth chemistry of felsic magmas., *Contrib. Mineral. Petrol., 94,* 304-316, 1986.

139. Reiss, Howard, *Methods of Thermodynamics,* 217 pp., Blaisdell Publishing Company, Waltham, Massachusetts, 1965.

140. Rovetta, M. R., Holloway, J. R., and Blacic, J. D., Solubility of hydroxl in natural quartz annealed in water at 900°C and 1.5 GPa, *Geophys. Res. Lett.,*

13, 145-148, 1986.

141. Ryerson, F. J., Diffusion measurements: experimental methods, *Methods Exp. Phys., 24A,* 89-130, 1987.

142. Ryerson, F. J., Durham, W. B., Cherniak, D. J., and Lanford, W. A., Oxygen diffusion in olivine: effect of oxygen fugacity and implications for creep, *J. Geophys. Res., 94,* 4105-4118, 1989.

143. Ryerson, F. J., and McKeegan, K. D., Determination of oxygen self-diffusion in åkermanite, anorthite, diopside, and spinel: Implications for oxygen isotopic anomalies and the thermal histories of Ca-Al-rich inclusions, *Geochim. Cosmochim. Acta, 58(17),* in press, 1994.

144. Sautter, V., Jaoul, O., and Abel, F., Aluminum diffusion in diopside using the $^{27}Al(p,\gamma)^{28}Si$ nuclear reaction: preliminary results, *Earth Planet. Sci. Lett., 89,* 109-114, 1988.

145. Shaffer, E. W., Shi-Lan Sang, J., Cooper, A. R., and Heuer, A. H., Diffusion of tritiated water in b-quartz, in *Geochemical Transport and Kinetics,* edited by Hofmann, A. W., Giletti, B. J., Yoder, H. S., Jr., and Yund, R. A., pp. 131-138, Carnegie Institution of Wash., Washington, 1974.

146. Sharp, Z. D., Giletti, B. J., and Yoder, H. S., Jr., Oxygen diffusion rates in quartz exchanged with CO_2, *Earth Planet. Sci. Lett., 107,* 339-348, 1991.

147. Shewmon, Paul G., *Diffusion in Solids,* 246 pp., Minerals, Metals & Materials Society, Warrendale, PA, 1989.

148. Smigelskas, A. D., and Kirkendall, E. O., Zinc diffusion in alpha brass, *Am. Inst.*

Min. Metal. Engrs. Trans., 171, 130-142, 1947.

149. Sneeringer, M., Hart, S. R., and Shimizu, N., Strontium and samarium diffusion in diopside, *Geochim. Cosmochim. Acta, 48,* 1589-1608, 1984.

150. Tiernan, R. J., Diffusion of thallium chloride into single crystals and bicrystals of potassium chloride, Ph.D. thesis, MIT, Cambridge, Massachusetts, 1969.

151. Trull, T. W., and Kurz, M. D., Experimental measurement of ^3He and ^4He mobility in olivine and clinopyroxene at magmatic temperatures, *Geochim. Cosmochim. Acta, 57,* 1313-1324, 1993.

152. Watson, E. B., Calcium diffusion in a simple silicate melt to 30 kbar, *Geochim. Cosmochim. Acta, 43,* 313-322, 1979a.

153. Watson, E. B., Diffusion of cesium ions in H_2O-saturated granitic melt, *Science, 205,* 1259-1260, 1979b.

154. Watson, E. B., Diffusion in fluid-bearing and slightly-melted rocks: experimental and numerical approaches illustrated by iron transport in dunite, *Contrib. Mineral. Petrol., 107,* 417-434, 1991a.

155. Watson, E. B., Diffusion of dissolved CO_2 and Cl in hydrous silicic to intermediate magmas, *Geochim. Cosmochim. Acta, 55,* 1897-1902, 1991b.

156. Watson, E. B., and Baker, D. R., Chemical diffusion in magmas: an overview of experimental results and geochemical applications, in *Physical Chemistry of Magmas, Advances in Physical Geochemistry, 9,* edited by Perchuk, L., and Kushiro, I., pp. 120-151, Springer-Verlag, New

York, 1991.

157. Watson, E. B., Harrison, T. M., and Ryerson, F. J., Diffusion of Sm, Ar, and Pb in fluorapatite, *Geochim. Cosmochim. Acta*, *49*, 1813-1823, 1985.

158. Watson, E. B., and Lupulescu, A., Aqueous fluid connectivity and chemical transport in clino-pyroxene-rich rocks, *Earth Planet. Sci. Lett.*, *117*, 279-294, 1993.

159. Watson, E. B., Sneeringer, M. A., and Ross, A., Diffusion of dissolved carbonate in magmas: experimental results and applications, *Earth Planet. Sci. Lett.*, *61*, 346-358, 1982.

160. Wendlandt, R. F., Oxygen diffusion in basalt and andesite melts: experimental results and

discussion of chemical versus tracer diffusion, *Contrib. Mineral. Petrol.*, *108*, 463-471, 1991.

161. Wendt, R. P., The estimation of diffusion coefficients for ternary systems of strong and weak electrolytes, *J. Phys. Chem.*, *69*, 1227-1237, 1965.

162. Winchell, P., The compensation law for diffusion in silicates, *High Temp. Sci.*, *1*, 200-215, 1969.

163. Yund, R. A., Diffusion in feldspars, in *Feldspar Mineralogy*, edited by Ribbe, P. H., pp. 203-222, Mineralogical Society of America, Washington, 1983.

164. Yund, R. A., Quigley, J., and Tullis, J., The effect of dislocations on bulk diffusion in

feldspars during metamorphism, *J. Metamorph. Geol.*, *7*, 337-341, 1989.

165. Yurimoto, H., Morioka, M., and Nagasawa, H., Diffusion in single crystals of melilite: I. oxygen, *Geochim. Cosmochim. Acta*, *53*, 2387-2394, 1989.

166. Zhang, Y., Stolper, E. M., and Wasserburg, G. J., Diffusion in rhyolite glasses, *Geochim. Cosmochim. Acta*, *55*, 441-456, 1991a.

167. Zhang, Y., Stolper, E. M., and Wasserburg, G. J., Diffusion of a multi-species component and its role in oxygen and water transport in silicates, *Earth Planet. Sci. Lett.*, *103*, 228-240, 1991b.